Regional Thermal Metamorphism and Deformation of the Sitka Graywacke, Southern Baranof Island, Southeastern Alaska

U.S. GEOLOGICAL SURVEY BULLETIN 1779

Regional Thermal Metamorphism and Deformation of the Sitka Graywacke, Southern Baranof Island, Southeastern Alaska

By ROBERT A. LONEY and DAVID A. BREW

U.S. GEOLOGICAL SURVEY BULLETIN 1779

DEPARTMENT OF THE INTERIOR
DONALD PAUL HODEL, Secretary

U.S. GEOLOGICAL SURVEY
Dallas L. Peck, Director

UNITED STATES GOVERNMENT PRINTING OFFICE, WASHINGTON : 1987

For sale by the
Books and Open-File Reports Section
U.S. Geological Survey
Federal Center, Box 25425
Denver, CO 80225

Library of Congress Cataloging-in-Publication Data

Loney, Robert Ahlberg, 1922–

Regional thermal metamorphism and deformation of the Sitka Graywacke, southern Baranof Island, southeastern Alaska.

U.S. Geological Survey Bulletin 1779
Bibliography
Supt. of Docs. No.: I 19.3: 1779
1. Metamorphism (Geology)—Alaska—Baranof Island. 2. Rock deformation—Alaska Baranof Island. 3. Sitka Graywacke (Alaska). I. Brew, David A. II. Title. III. Series.
QE75.B9 No. 1779 557.3 s 87–600001
[QE475.A2] [552'.4'097982]

CONTENTS

FIGURES

TABLES

Regional Thermal Metamorphism and Deformation of the Sitka Graywacke, Southern Baranof Island, Southeastern Alaska

By Robert A. Loney *and* David A. Brew

Abstract

Southern Baranof Island is underlain by at least 1,200 km^2 of regional thermally metamorphosed rocks, making it one of the largest regions of such metamorphism reported to date. Turbidites of the Sitka Graywacke of Late Jurassic and Early Cretaceous age belonging to the flysch facies of the Chugach terrane were metamorphosed to albite-epidote hornfels, hornblende hornfels, amphibolite, and perhaps pyroxene hornfels facies by Tertiary (about 42 to 47 Ma) granitic plutons. The protolith was compositionally limited, and a full sequence of metamorphic minerals documenting the temperature increase is present; further studies could establish the detailed pressure-temperature-composition history of the region.

Prior to the regional thermal metamorphism, the Sitka Graywacke was dynamothermally metamorphosed to prehnite-pumpellyite-metagraywacke or lower greenschist facies. This event was synchronous with regional folding with northwest-striking subvertical axial planes and axial-plane foliation and axial orientations ranging from a moderate southeast plunge through horizontal to a moderate northwest plunge. Two generations of folds and foliations of about the same style and axial orientation are actually present, but because of their similarity they cannot be separated consistently and are therefore considered two phases of a single deformation. Subsequent emplacement of the plutons had little effect on the structural geometry.

Based on major-oxide and trace-element analyses of 20 specimens from throughout the region, there appear to be no systematic changes in composition from lower to higher grades. The analyses show that the coarse-grained metagraywackes are semipelites, and that the fine-grained metamudstones are pelites that are compositionally within the system SiO_2-Al_2O_3-MgO-FeO-K_2O-H_2O.

Individual aureoles are zoned, in general, inward from low to high temperature and perhaps from low to higher pressure. Local synkinematic metamorphism produced intensely foliated and lineated schists subparallel to the preexisting general structural orientation, and these schists are interpreted to be related to an early phase of the intrusive event. Seven previously mapped metamorphic mineral zones were evaluated relative to reaction isograds and bulk compositional control based on mineral assemblages in pelitic schists. Zones L1 to L3 are the biotite zone, the L3-L4 boundary is the garnet isograd, L4 is the garnet zone, the L4-H1 boundary is the andalusite-cordierite-biotite isograd, H1 and H2 are the andalusite-cordierite-biotite zone, the H2-H3 boundary is the sillimanite isograd, and H3 is the sillimanite zone; in addition, a higher garnet-cordierite zone was newly recognized. The restricted occurrence of staurolite is probably due to the generally inappropriate bulk composition.

The sequence of mineral assemblages in the aureoles was used to define a pressure-temperature gradient that ranges from about 3.9 kbars at 550 °C to about 4.4 kbars at 790 °C. These pressures are equivalent to a depth of metamorphism of from 13.6 to 15.4 km.

INTRODUCTION

Previous geologic studies on Baranof Island (Loney and others, 1975, p. 62-65, 73-85; fig.1) indicated that at least 1,200 km^2 of pelitic and semipelitic rocks had been subjected to clearly zoned regional thermal metamorphism associated with granitic plutons of Tertiary age (42-47 Ma, Loney and others, 1967). Inasmuch as this is one of the world's largest known areas of regional metamorphism (Miyashiro, 1973; Turner, 1981), we have reexamined the original interpretations, which were based on about 120 thin sections and reconnaissance mapping (Loney and others, 1975) in light of 20 additional specimens and chemical analyses; our goals in this report are to summarize the present understanding of this unique region and to encourage more detailed studies. Our study is limited both by the reconnaissance nature of the fieldwork and by our lack of detailed compositional data on the minerals in the different assemblages; we have nevertheless pressed the interpretations as far as possible lacking such information.

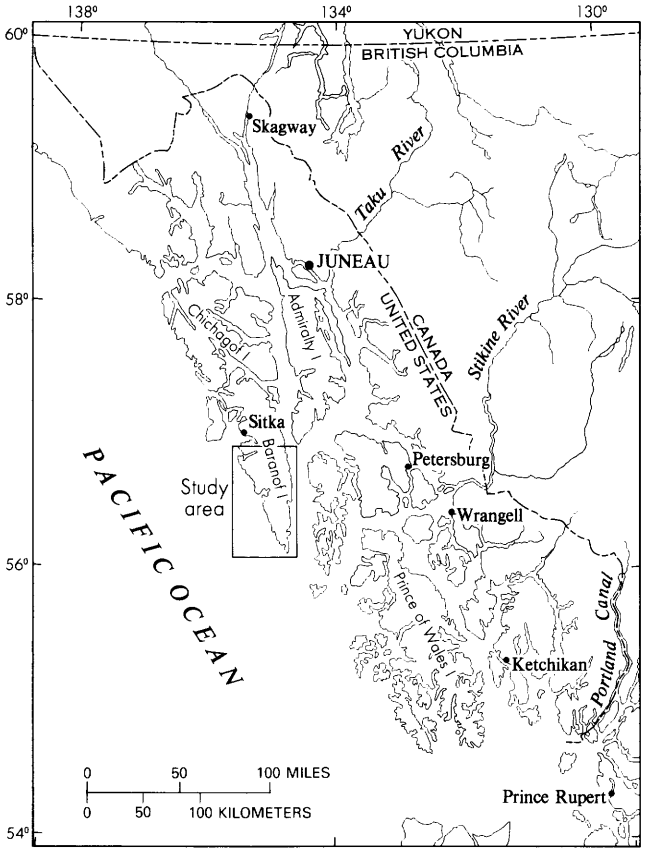

Figure 1. Index map of southeastern Alaska, showing the southern Baranof Island study area.

The protolith of the metamorphic rocks is the Sitka Graywacke of Late Jurassic and Early Cretaceous age (Loney and others, 1975). It consists dominantly of turbidites, probably all derived from the same provenance terrane, that have consistent textures, mineralogy, and (as is shown here) a restricted range of chemical composition. Prior to the intrusion of the granitic bodies, the rocks were folded and underwent low-grade regional metamorphism, resulting in a homogeneous structural and lithologic environment. The granitic bodies were generally passively intruded both along and transverse to the dominant north-northwest-trending older structures, which makes it possible to study metamorphic changes along and across the general strike of the compositional layers.

The field studies suggested that the turbidites had simple and consistent chemical compositions, and this in turn suggested that it would be possible to test if the metamorphism were isochemical. To do this (1) all but one of the seven different zones defined in our previous investigations were revisited and sampled to obtain both the coarsest grained rock type (generally sandstone protolith) and the finest grained type present (generally mudstone protolith); (2) the samples were analyzed for 10 major elements by X-ray fluorescence techniques, for FeO by chemical techniques, and for 45 trace elements by emission-spectrographic techniques; and (3) the results of the chemical analyses were analyzed statistically for central tendency and dispersion, with the sandstones and mudstones treated separately. In general, the analyses show the sandstones (metagraywackes) to be uniformly semipelitic and the mudstones to be uniformly pelitic.

The mineral assemblages resulting from the temperature and pressure changes associated with the Tertiary intrusions indicate that albite-epidote hornfels, hornblende hornfels, amphibolite, and perhaps transitional pyroxene hornfels facies (Turner, 1981) are present. The wide distribution of pelitic rocks of uniform composition resulted in the wide development of mineral assemblages in the SiO_2-Al_2O_3-MgO-FeO-K_2O-H_2O system (Thompson, 1957). This uniformity allowed construction of coherent mineral-assemblage zones, which were evaluated relative to isograds and to model metamorphic reactions. These zones were correlated with the previously mapped metamorphic mineral zones (see fig. 5 and tables 1 and 6; Loney and others, 1975). In a discussion section, the pressure-temperature (P-T) gradient of the Baranof metamorphic facies series is interpreted with regard to the sequence of mineral assemblages in this region. At the present time, both our lack of detailed mineral composition data and the unsolved experimental problems prevent certain estimates of P-T conditions. Nevertheless, we have used the available information to infer ranges for those conditions.

Acknowledgments

We wish to thank G.R. Himmelberg for his review of the revised manuscript and for helpful discussions on metamorphic petrology; A.B. Till, B.R. Johnson, and two anonymous reviewers for their perceptive reviews of the original manuscript; and two anonymous reviewers of the revised manuscript for some helpful comments. We also acknowledge the helpful advice of L.S. Hollister (an associate editor for the Bulletin of the Geological Society of America), who enlightened us on the proper vehicle for the publication of reconnaissance studies of metamorphic terranes.

GEOLOGIC SETTING

The protolith for the metamorphic rocks consisted of semipelitic and pelitic sediments: very thick bedded lithic and arkosic wacke, interbedded thin- to medium-bedded wacke and shale, and rhythmically thin-bedded wacke and shale turbidite. Metavolcanic rocks and metacherts occur sparsely in the southeastern part of Baranof Island. All these rocks are part of the Sitka Graywacke (Loney and others, 1975). Based on the study by Zuffa and others (1980) of the rock-fragment component in selected graywacke samples from southern Baranof Island, the clasts were probably derived from a terrane composed dominantly of volcanic rocks but also containing a significant amount of sedimentary rocks and lesser

amounts of plutonic and low-grade metamorphic rocks. The earlier study (Loney and others, 1975) concluded that, compositionally, the graywackes are (in order of decreasing abundance) feldspathic, lithic, and arkosic (Gilbert, in Williams and others, 1954). They typically contain 10-30 percent potassium feldspar (orthoclase and minor microcline), 5-30 percent plagioclase (oligoclase to andesine), 30-60 percent lithic fragments, and minor amounts of myrmekite, biotite, muscovite, apatite, augite, hypersthene, zircon, garnet, and hornblende. The shale or argillite beds interbedded with the graywacke are compositionally similar to the graywacke matrix material.

Sometime prior to the contact metamorphism and probably accompanying the structural events described below, the Sitka Graywacke underwent low-grade regional dynamothermal metamorphism. In general, the mineral assemblages related to this "background" metamorphism are indicative of the prehnite-pumpellyite-metagraywacke facies (Turner, 1981), but in many places they are indistinguishable from those of the lower greenschist facies. These lower grade rocks are characterized by widespread chlorite.

STRUCTURE

The rocks of southern Baranof Island have been folded twice (F_1 and F_2); evidence for these episodes is found only in the vicinity of the Tertiary plutons. Folds (B_1) in bedding (S) have northwest-striking subvertical axial planes and axial-plane foliation (S_1) and axial orientations ranging from a moderate southeast plunge through horizontal to a moderate northwest plunge. The metamorphic terrane is divided into two structural domains (fig. 2): domain I, in which B_1 folds plunge mainly to the northwest, and domain II, in which they plunge mainly to the southeast. The southeast-plunging domain contains a number of northwest-plunging fold axes that are concentrated largely in four narrow eastward-trending subdomains too small to show with separate plots but that are outlined within the domain (dashed regions in fig. 2).

The second folding episode (F_2) also affected these rocks, and the strong preferred orientation of planar and linear elements in these two domains is in part due to a pronounced S_2 foliation that maintains a remarkably uniform orientation throughout the metamorphic terrane. The S_2 foliation cuts the B_1 folds and S_1 foliation and appears to be subparallel to axial planes of B_2 folds that deform bedding and S_1 foliation. In contrast to the commonly cataclastic nature of the S_1 foliation, the S_2 foliation is defined mainly by the planar preferred orientation of micaceous minerals and by strain-slip cleavage.

Although there are two generations of folds and foliation in the metamorphic terrane, the geometry of the planar and linear structures of both generations is about the same, and they share almost the same axis of folding. The two generations indicate either two distinct phases of the same episode of compression or two distinct episodes of compression with similar orientations. Because of their close similarity of orientation, the two generations were not consistently separated in the field. They are here considered two phases of a single deformation that occurred after the deposition of the Sitka Graywacke in Late Jurassic and Early Cretaceous time and either with or before the Tertiary plutonism.

The areas in which these deformational effects are most apparent have been mapped as "lineated, schistose, and semischistose graywacke and slate" on figure 3. The lineations in these areas consist of mineral alignments marking S intersections, very small scale folds or crenulations, and local rodding. The schistosity varies from a close-spaced cleavage to a well-developed platy metamorphic mineral schistosity. The contacts of this lineated terrane with the adjacent nonlineated hornfels are gradational over a few hundred meters, except in the area near Whale Bay, where sporadic lineations occur over a broad area.

Local recrystallization of the S_1 cataclastic foliation and synchronous growth of micaceous minerals along the S_2 foliation show that the metamorphic conditions related to the Tertiary plutonism in southern and eastern Baranof Island started sometime during the F_2 folding (Loney and others, 1975, p. 63, 64). The metamorphism appears to have continued after the F_2 folding stopped, as indicated in the inner zones of some contact aureoles, where metamorphic crystallization has tended to obscure the F_2 structures. The Tertiary plutons appear to be postkinematic because they are distinctly crosscutting and not highly foliated. It is possible, therefore, that the metamorphism that occurred during the F_2 folding preceded the actual intrusion of the plutons to their present level.

METAMORPHISM

General Description

The aureoles developed in the Sitka Graywacke by the Tertiary granitic rocks are zoned, in general, inward from low to high temperature. The pressure of metamorphism of the low-temperature, outer part (albite-epidote hornfels and (or) greenschist facies) was low, whereas the pressure of the high-temperature, inner zones may have been higher (that is, transitional between hornblende hornfels facies and amphibolite facies; Turner, 1981). The distribution of the mineral assemblages indicative of this zonation is complicated, varying from pluton to pluton and, around the Crawfish Inlet, varying from the north side to the south. The area of concern in this study is on the south side of the pluton at Crawfish Inlet (table 1; fig. 3). The aureole here is broad and contains the best developed zoning, which is interpreted to have been produced by a single episode of thermal metamorphism. The apparent higher pressures suggested by the mineral assemblages closer to the plutons may have been induced by local effects of the diapirlike intrusions. This progressive low- to high-temperature, low- to medium-pressure metamorphism was accompanied and closely preceded by the deformation (F_2) described earlier.

The areal distribution of the lineated and schistose rocks is related to the exposed plutons and

their contact metamorphic aureoles in that similar rocks do not occur elsewhere within the Sitka Graywacke, even where isolated plutons are present. The lineated rocks do not occur immediately adjacent to igneous masses except locally near the pluton at Redfish Bay and at Whale Bay, but they do, in general, form a band connecting the plutons at Crawfish Inlet and at Redfish Bay. The configuration of the metamorphic zones shows a close relationship to the pluton at Redfish Bay and a loose relationship to the pluton at Crawfish Inlet (fig. 3), and most of the lineated terrane is directly along and to the southeast of the shortest distance connection between the two plutons. All of the mapped igneous-metamorphic rock contacts on the south and southwest sides of the pluton at Crawfish Inlet are steep, but several small cupolas indicate the probable presence of a larger granitic body at depth.

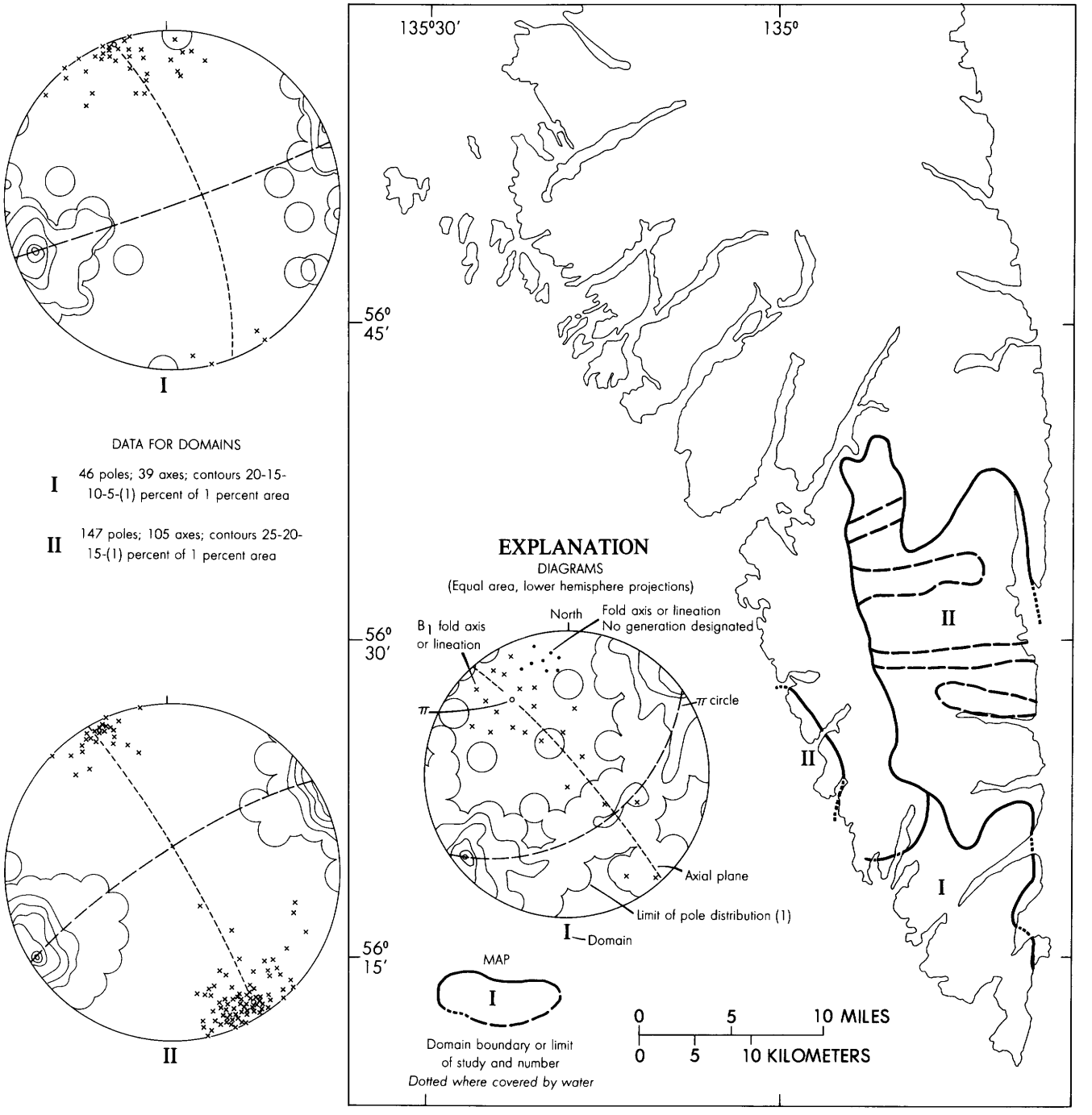

Figure 2. Southern Baranof Island, showing structural domains and geometry of bedding, foliation, fold axes, and lineations (from Loney and others, 1975, pl. 3). Dashed boundaries indicate regions containing northwest-plunging fold axes within the southeast-plunging domain.

Although not conclusive, these relationships suggest that the two igneous masses are connected at depth and that the lineated terrane was produced during the emplacement of this inferred large igneous body. These suggestions are supported by the abruptness of the gradational transition between lineated and nonlineated terranes, and by the greater distance between the metamorphic isograds south of the pluton at Crawfish Inlet than north. As speculation, it is possible that this inferred concealed body is a pluton intruded during F_2 folding that is nowhere exposed. Later, after the folding had ceased, the presently exposed plutons intruded through it to their present level. Alternatively, the inferred body may represent an early phase of a series of continuous intrusions that culminated in the exposed plutons, or it may represent a magma chamber from which the later magma moved upward. In any case, the lineated and schistose unit is interpreted to be a part of the contact aureole of an unexposed, slightly(?) earlier, synkinematic pluton. If this pluton is the initial phase of the Tertiary plutonism, as is suggested above, then the F_2 folding died out during the Tertiary plutonism. If this interpretation is correct, the lineated terrane lies in the southeastward-dipping roof of a large concealed pluton and is analogous to the southward-dipping, deeply eroded roof of the pluton elsewhere on Baranof Island at Kasnyku Lake (Loney and others, 1975, p. 85-87).

Whole-Rock Composition

Before attempting to apply Thompson's (1957) analysis of mineral assemblages in pelitic schists, we first examine the bulk compositions of rocks of the aureole and compare them with those of typical pelitic schist. The 20 samples collected for chemical analysis were studied petrographically, but not all the mineral assemblages described by Loney and others (1975) were found in samples collected for this chemical study. Brief descriptions of the samples are given in tables 2 and 3. The mineral assemblages in all the samples are compatible with those in the biotite to sillimanite zones of the present work (zones L1 to H3 as defined by the previous work), even though diagnostic minerals were lacking in some specimens.

With the one exception described below and with due consideration of the limited number of samples available, the major oxides of the coarse- and fine-grained samples fall respectively into two distinct groups. Inspection of the data (tables 2 and 3) and plots (not included here) for the oxides compared with the metamorphic zones shows (1) the general uniformity of oxide content within each group, and (2) the absence of systematic changes between the higher and lower metamorphic zones.

The uniformity within each group is confirmed by the statistical analysis (table 4). The fine-grained specimens are significantly lower in SiO_2 and significantly higher in Al_2O_3, MgO, FeO, and TiO_2 than are the coarse-grained samples. The interpretation of the apparent absence of systematic changes between the zones is severely limited by the low (1 or 2) number of samples in each zone.

The exception referred to above concerns specimen 79DB178B (table 3); it was collected as a fine-grained rock interlayered with a coarser grained rock and was thought to represent a mudstone originally interlayered with graywacke. The major-oxide composition of 79DB178B is clearly closer to that of the coarse-grained rocks, and petrographic study suggests that the sample was originally a fine-grained sandstone that has been "milled" to finer grain size, rather than being an original mudstone. For these reasons, the sample was not included in the statistical analysis.

The trace-element compositions of the coarse- and fine-grained rocks (tables 2 and 3) are not significantly different, and inspection of the data shows no systematic change from the lower metamorphic zones to the higher.

The foregoing discussion indicates that the interbedded metagraywacke and metamudstone units are remarkably uniform in composition throughout the aureoles. The bulk composition of fine-grained rocks compares favorably with the mean values for the compositions of metamorphic rocks of pelitic origin given by Mehnert (1969). For example, his mean values for SiO_2 range from 59.64 to 61.18 percent (avg 60.43 percent); for Al_2O_3 from 16.4 percent to 17.41 percent (avg 16.90 percent); and for K_2O from 3.25 percent to 4.14 percent (avg 3.62 percent). Finally, the thinly bedded nature of these rocks ensures that both pelitic and semipelitic rocks are distributed more or less uniformly throughout the aureole.

Garnet Composition

Although the garnets are known to be zoned (on the basis of primitive microprobe studies made in the 1960's), we have no reliable compositional data on the zoning. The available bulk composition information listed in table 5 is intended only to show that the garnets from pelitic schists (62ABd149 and 62ABd152, containing 91.6 and 86.5 percent almandine + pyrope, respectively) have a composition much more appropriate for the AFM projections (Thompson, 1957) than do those from semipelitic rocks (62ABd147, 66.4 percent almandine + pyrope).

Metamorphic Isograds and Zones

Loney and others (1975, p. 80-81) mapped metamorphic zones (L1 to H3) on the south side of the pluton at Crawfish Inlet and around the Redfish Bay pluton (fig. 3). The mineral assemblages upon which these zones are based and the inferred facies were discussed in detail by these authors and are summarized, together with the zones as defined in this paper, in table 1. The present work evaluates the earlier defined zones relative to reaction isograds or bulk-composition controls, and the map (fig. 3) shows only those zone boundaries that are true isograds in the sense that they represent changes of mineral facies diagrams.

To minimize the effects of bulk composition, Thompson (1957) proposed that isograds be defined on the basis of discontinuous reactions, and as an aid to

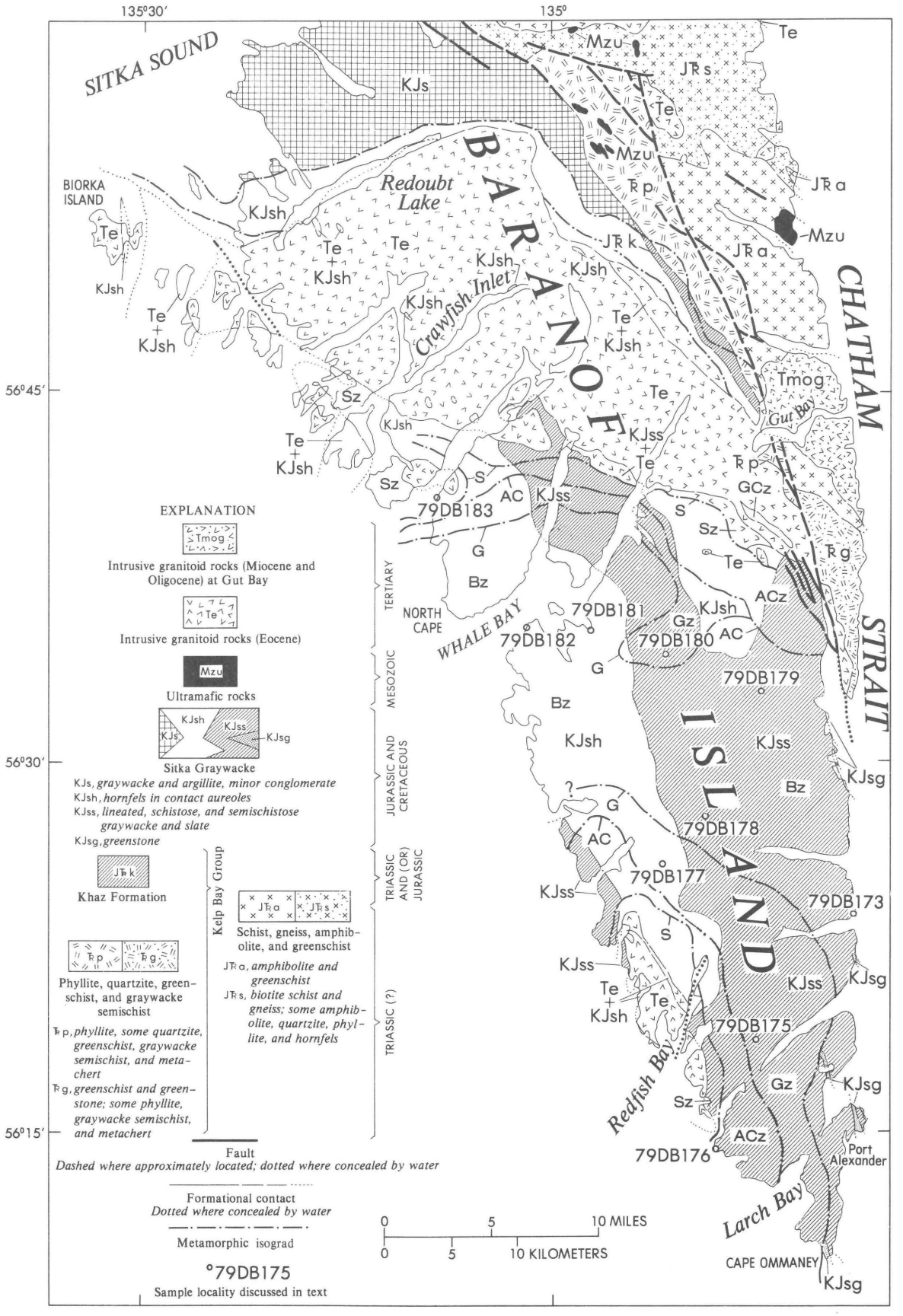
135°30′
135°
56°45′
56°30′
56°15′
SITKA SOUND
BIORKA ISLAND
BARANOF ISLAND
CHATHAM STRAIT
Redoubt Lake
Crawfish Inlet
Gut Bay
NORTH CAPE
WHALE BAY
Redfish Bay
Larch Bay
Port Alexander
CAPE OMMANEY
79DB183
79DB182
79DB181
79DB180
79DB179
79DB178
79DB177
79DB176
79DB175
79DB173
EXPLANATION
Intrusive granitoid rocks (Miocene and Oligocene) at Gut Bay
Intrusive granitoid rocks (Eocene)
Ultramafic rocks
Sitka Graywacke
KJs, graywacke and argillite, minor conglomerate
KJsh, hornfels in contact aureoles
KJss, lineated, schistose, and semischistose graywacke and slate
KJsg, greenstone
Khaz Formation
Kelp Bay Group
Schist, gneiss, amphibolite, and greenschist
JTRa, amphibolite and greenschist
JTRs, biotite schist and gneiss; some amphibolite, quartzite, phyllite, and hornfels
Phyllite, quartzite, greenschist, and graywacke semischist
TRp, phyllite, some quartzite, greenschist, graywacke semischist, and metachert
TRg, greenschist and greenstone; some phyllite, graywacke semischist, and metachert
TERTIARY
MESOZOIC
JURASSIC AND CRETACEOUS
TRIASSIC AND (OR) JURASSIC
TRIASSIC (?)
Fault
Dashed where approximately located; dotted where concealed by water
Formational contact
Dotted where concealed by water
Metamorphic isograd
°79DB175
Sample locality discussed in text
0 5 10 MILES
0 5 10 KILOMETERS

Table 1. Metamorphic mineral zones in the aureoles south of Crawfish Inlet as defined by Loney and others (1975, p. 79-81) and their correlation with isograds and zones in this paper

[FA, first appearance; A, absence. Identification: H, hand lens; P, petrographic methods; An_{10+} or An_{10-}, plagioclase composition. Rocks also contain quartz, muscovite, biotite, and plagioclase]

This paper	Loney and others (1975)	
Biotite zone (Bz)	L1	FA biotite H; An_{10-}
	L2	FA epidote and tourmaline P; An_{10-}
	L3	A chlorite and calcite P; An_{10-}
Garnet isograd ----------		
Garnet zone (Gz)	L4	FA garnet + cordierite P; An_{10+}
Andalusite-cordierite-biotite isograd----------		
Andalusite-cordierite-biotite zone (ACz)	H1	FA andalusite H and garnet H; An_{10+}
	H2	FA staurolite H; An_{10+}
Sillimanite isograd----------		
Sillimanite zone (Sz)	H3	FA sillimanite + orthoclase P; An_{10+}
Garnet-cordierite isograd----------		
Garnet-cordierite zone (GCz)		Not recognized

studying these reaction isograds (Winkler, 1979, p. 66) he introduced the AFM projection of the "ideal" pelitic system SiO_2-Al_2O_3-MgO-FeO-K_2O-H_2O. On the AFM projection, discontinuous reactions may be indicated by distinct changes in the tieline configuration without necessarily implying that the reaction actually occurred in the rocks concerned.

The mineral assemblages from the rocks of the aureole appropriate to the AFM projection are listed in table 6. In addition to the minerals listed, all assemblages contain quartz and muscovite, and they may also contain plagioclase, orthoclase, and accessory ilmenite, magnetite, graphite, zircon, apatite, tourmaline, epidote, and sphene. All phases in an assemblage are inferred to be in equilibrium on the basis of textural criteria. The order in which minerals are listed has no significance. The compositions of the two analyzed garnets from pelitic schists (table 5) are plotted on a schematic AFM projection (fig. 4). Also plotted on this projection is the field of compositions for the pelitic schists analyzed (table 3), which was used to control the mineral assemblage construction. According to Thompson (1957), rock compositions may be plotted on the AFM projection provided that the content of the mineral phases not appearing in the projection are first subtracted from the bulk composition. Plagioclase is the only such mineral of significance in these rocks; therefore, an amount of Al_2O_3 equivalent to the amount of CaO and Na_2O was subtracted from each rock analysis plotted on the AFM projection (fig. 4).

AFM diagrams constructed from observed and compatible mineral assemblages (table 6) are shown in figure 5. The first appearance of garnet marks the garnet isograd and the boundary between the biotite and the garnet zones (tables 1 and 6; fig. 5A). The garnet isograd cannot be modeled by a discontinuous reaction, and we lack the critical textural evidence to work out the details of the reaction. However, it is likely the formation of garnet was related to continuous reactions such as those given by Chakraborty and Sen (1967),

$$\text{Chl} + \text{Bt} + \text{Qtz} = \text{Gt} + \text{Bt} + \text{W}, \quad (1)$$

and by Thompson (1976),

$$\text{Chl} + \text{Mu} + \text{Qtz} = \text{Gt} + \text{Bt} + \text{W}. \quad (2)$$

The first occurrence of garnet, then, is probably bulk compositionally dependent, and the relatively widespread occurrence of the garnet-biotite-chlorite assemblage reflects the relatively uniform bulk composition of the pelitic rocks of the garnet zone.

Although generally a minor constituent of the garnet zone, rocks containing the assemblage chlorite-biotite-cordierite form a relatively wide (4 km maximum), vaguely defined zone east of Redfish Bay in which garnet-bearing rocks are sparse. A reevaluation of the evidence in this area resulted in a major widening of the original garnet zone at the expense of the andalusite-cordierite-biotite zone to the west (fig. 3).

Figure 3. Southern Baranof Island, showing major geologic units, metamorphic isograds and zones related to the Crawfish Inlet and Redfish Bay plutons, and locations of samples analyzed. Bz, biotite zone; G, garnet isograd; Gz, garnet zone; AC, andalusite-cordierite-biotite isograd; ACz, andalusite-cordierite-biotite zone; S, sillimanite isograd; Sz, sillimanite zone; GCz, garnet-cordierite zone. (Modified from Loney and others, 1975, fig. 25.)

Table 2. Major oxide and semiquantitative spectrographic analyses of metamorphosed coarse-grained rocks of the Sitka Graywacke, southern Baranof Island, Alaska

[X-ray spectroscopic analyses by L. Estos and S. Ramage. FeO and powder density determinations by P. Klock. Emission spectrographic analyses by C. Heropoulos; data reported by procedure described in Meyers and others (1961). See table 1 for zone abbreviations. Concentrations below procedural detection limits are indicated by the less than (<) values. Trace elements looked for but not detected (minimum detection limit, in parts per million, in parentheses): Ag (0.7), As (100.0), Au (7.0), Bi (7.0), Cd (7.0), Ce (50.0), Eu (1.0), Ge (7.0), Hf (50.0), In (1.50), Li (100.0), Mo (2.0), Nd (20.0), Pd (1.0), Pr (20.0), Pt (5.0), Re (7.0), Sb (15.0), Sm (50.0), Ta (50.0), Te (300.0), Th (150.0), Tl (3.0), U (150.0), W (10.0)]

Zone	Bz(L1)	Bz(L2)		Bz(L3)		Gz(L4)			ACz(H2)	Sz(H3)
Specimen	79DB182A	79DB173A	79DB181A	79DB178A	79DB179A	79DB177A	79DB180A	79DB175A	79DB176A	79DB183A
Lat (56° N.)	35'22"	23'50"	34'24"	28'07"	32'40"	25'13"	33'40"	20'47"	14'04"	40'30"
Long (134° W.)	01'52"	36'11"	56'36"	48'56"	46'54"	50'50"	50'37"	40'17"	47'43"	08'25"
Major oxide analyses (weight percent)										
SiO_2	70.37	70.63	69.34	66.42	65.97	71.69	68.39	67.17	68.78	69.97
Al_2O_3	14.86	13.38	14.62	15.50	15.76	14.27	15.78	14.44	15.18	14.61
Fe_2O_3	.74	.71	.50	.86	.87	.58	.62	.77	.53	.47
FeO	2.97	3.61	3.02	4.34	3.80	2.81	3.64	4.07	3.73	2.96
MgO	1.65	1.90	1.59	2.42	2.44	1.54	2.15	2.39	2.11	1.68
CaO	2.00	2.54	2.19	2.21	2.36	2.16	1.89	2.91	1.69	1.98
Na_2O	3.97	3.42	3.69	3.97	3.47	3.64	3.07	3.52	1.88	4.09
K_2O	2.09	1.85	2.39	1.89	2.62	1.83	2.42	1.82	3.81	2.44
TiO_2	.52	.58	.50	.75	.69	.50	.58	.68	.50	.49
P_2O_5	.10	.13	.10	.15	.13	.11	.10	.13	.11	.11
MnO	.06	.07	.05	.08	.06	.06	.07	.08	.07	.06
Total	99.33	98.82	97.99	98.59	98.17	99.19	98.71	97.98	98.39	98.86
Powder density	2.72	2.72	2.80	2.76	2.76	2.72	2.72	2.72	2.84	2.72
Semiquantitative spectrographic analyses (parts per million)										
B	10	5	10	2	5	10	15	15	7	20
Ba	700	700	700	700	1500	500	700	500	1500	1000
Be	1.5	1	1	1	1.5	1	1	1	2	1
Co	10	20	10	10	7	7	10	20	10	15
Cr	30	30	30	30	30	30	20	50	20	50
Cu	30	10	20	20	20	20	30	30	20	50
Ga	20	20	20	20	30	20	20	30	30	30
La	70	30	30	50	50	50	50	50	70	30
Mn	500	700	300	500	500	500	500	1000	500	500
Nb	10	10	15	7	15	20	15	10	20	15
Ni	15	20	15	10	7	15	10	30	20	20
Pb	30	20	30	20	20	30	30	50	30	30
Sc	15	20	10	15	15	15	15	20	15	20
Sn	3	< 2	5	3	3	3	3	< 2	5	5
Sr	300	500	300	300	700	300	300	300	300	300
V	150	150	100	150	150	100	100	150	100	200
Y	15	20	15	15	15	15	15	20	20	15
Yb	2	3	2	2	2	2	2	3	3	2
Zn	70	100	70	70	100	70	100	150	100	100
Zr	100	100	70	100	70	200	70	150	100	100

Specimen descriptions:
79DB182A.Fine-grained epidote-opaque-muscovite-biotite-plaglioclase-quartz metagraywacke.
79DB173A.Fine- to very fine grained calcite-chlorite-epidote-biotite-plagioclase-quartz semischist.
79DB181A.Fine-grained calcite-opaque-muscovite-biotite-plagioclase-quartz metagraywacke.
79DB178A.Fine- to very fine grained epidote-opaque-muscovite-biotite-plagioclase-quartz semischist.
79DB179A.Fine- to very fine grained ilmenite-muscovite-biotite-plagioclase-quartz semischist.
79DB177A.Fine-grained tourmaline-epidote-opaque-muscovite-biotite-plagioclase-quartz semischist.
79DB180A.Fine-grained tourmaline-epidote-opaque-muscovite-biotite-plagioclase-quartz semischist.
79DB175A.Fine- to very fine grained andalusite(?)-muscovite-ilmenite-tourmaline-epidote-garnet-biotite-plagioclase-quartz semischist.
79DB176A.Fine- to very fine grained opaque-muscovite-biotite-plagioclase-quartz schist.
79DB183A.Fine-grained K-feldspar-opaque-muscovite-biotite-plagioclase-quartz hornfels/metagraywacke.

Table 3. Major oxide and semiquantitative spectrographic analyses of metamorphosed fine-grained rocks of the Sitka Graywacke, southern Baranof Island, Alaska

[X-ray spectroscopic analyses by L. Espos and S. Ramage. FeO and powder density determinations by P. Klock. Emission spectrographic analyses by C. Heropoulos; data reported by procedure described in Meyers and others (1961). See table 1 for zone abbreviations. Concentrations below procedural detection limits are indicated by the less than (<) values. Trace elements looked for but not detected (minimum detection limit, in parts per million, in parentheses): Ag (0.70), As (100.0), Au (7.0), Bi (7.0), Cd (7.0), Ce (50.0), Eu (1.0), Ge (7.0), Hf (50.0), In (1.50), Li (100.0), Mo (2.0), Nd (20.0), Pd (1.0), Pr (20.0), Pt (5.0), Re (7.0), Sb (15.0), Sm (50.0), Ta (50.0), Te (300.0), Th (150.0), Tl (3.0), U (150.0), W (10.0)]

Zone	Bz(L1)	Bz(L2)		Bz(L3)		Gz(L4)			ACz(H2)	Sz(H3)
Specimen	79DB182B	79DB173B	79DB181B	79DB178B	79DB179B	79DB177B	79DB180B	79DB175B	79DB176B	79DB183B
Lat (56° N.)	35'22"	23'50"	34'24"	28'07"	32'40"	25'13"	33'40"	20'47"	14'04"	40'30"
Long (134° W.)	01'52"	38'11"	56'36"	48'56"	46'54"	50'50"	50'37"	40'17"	47'43"	08'25"
Major oxide analyses (weight percent)										
SiO_2	63.36	61.03	60.39	70.59	60.04	59.36	60.42	62.63	63.61	59.93
Al_2O_3	17.09	16.88	18.32	13.93	18.97	17.80	18.66	17.87	17.80	18.64
Fe_2O_3	.70	1.13	.80	.70	.82	.97	1.12	.61	.89	.85
FeO	4.75	5.64	5.51	3.74	4.75	5.35	4.18	5.34	5.22	4.87
MgO	2.78	2.97	3.03	2.09	3.03	3.49	2.75	2.92	3.01	2.68
CaO	2.58	2.77	2.44	1.75	2.62	3.00	2.17	2.46	2.00	2.05
Na_2O	2.83	2.38	2.50	2.02	3.60	2.70	2.29	2.63	2.64	2.78
K_2O	3.41	2.95	3.95	2.60	2.97	2.38	3.62	3.48	3.26	4.39
TiO_2	.75	.91	.78	.68	.84	.81	.89	.77	.80	.76
P_2O_5	.19	.21	.17	.13	.13	.21	.17	.18	.21	.16
MnO	.08	.10	.07	.06	.08	.11	.08	.12	.09	.09
Total	98.52	96.97	97.96	98.29	97.85	96.18	96.35	99.01	99.53	97.20
Powder density	2.76	2.76	2.84	2.76	2.76	2.88	2.76	2.76	2.84	2.76
Semiquantitative spectrographic analyses (parts per million)										
B	20	15	30	15	7	30	50	30	70	20
Ba	1000	1000	1500	1500	1000	1000	1000	700	1000	1000
Be	1	1.5	1	1.5	1	1	< 0.7	1.5	1.5	1
Co	10	30	15	20	10	15	7	30	15	15
Cr	30	70	50	50	50	30	50	50	50	50
Cu	30	70	70	100	50	70	30	70	70	50
Ga	20	30	30	20	30	30	30	30	30	30
La	50	70	30	< 7	20	50	50	70	50	30
Mn	700	1000	500	500	500	700	500	1500	700	500
Nb	15	10	10	10	10	10	15	10	15	15
Ni	20	50	30	30	10	20	10	50	30	20
Pb	30	30	30	20	30	30	20	50	20	30
Sc	20	30	20	15	15	15	20	20	15	20
Sn	3	< 2	7	3	3	5	3	< 2	5	5
Sr	200	300	300	200	300	300	300	300	300	300
V	200	200	200	150	200	200	150	200	200	200
Y	15	30	20	15	15	15	15	30	15	15
Yb	2	5	2	2	2	3	2	3	3	2
Zn	100	150	100	100	100	150	70	200	100	100
Zr	70	200	70	70	100	70	70	150	70	100

Specimen descriptions:

79DB182B. Very fine grained opaque-muscovite-epidote-plagioclase-quartz-biotite metamudstone.
79DB173B. Very fine grained epidote-ilmenite-biotite-chlorite(?)-plagioclase-quartz phyllite.
79DB181B. Very fine grained tourmaline-ilmenite-plagioclase-quartz-biotite-muscovite metamudstone.
79DB178B. Fine- to very fine grained opaque-muscovite-biotite-plagioclase-quartz semischist.
79DB179B. Fine- to very fine grained tourmaline-epidote-ilmenite-muscovite-biotite-plagioclase-quartz schist.
79DB177B. Very fine grained ilmenite-muscovite-biotite-plagioclase-quartz schist.
79DB180B. Very fine grained tourmaline-muscovite-ilmenite-biotite-quartz schist.
79DB175B. Fine- to very fine grained epidote-garnet-opaque-chlorite-muscovite-biotite-plagioclase-quartz semischist.
79DB176B. Very fine grained staurolite-garnet-muscovite-biotite-plagioclase-quartz schist.
79DB183B. Very fine grained opaque-cordierite(?)-plagioclase-quartz-muscovite-biotite schist.

The assemblage chlorite-biotite-cordierite requires a magnesian bulk composition (Burnell and Rutherford, 1984). Hess' (1969) petrogenetic grid shows that the assemblage chlorite-biotite-cordierite can be associated in the same P-T fields as the garnet-zone assemblage chlorite-biotite-garnet, and therefore it may be considered compatible with the garnet zone in the absence of andalusite and staurolite.

The andalusite-cordierite-biotite isograd is marked by the first appearance of andalusite and by the disappearance of chlorite (figs. 5A and 5B; table 6). The breaking of the chlorite-garnet tieline commonly involves the appearance of staurolite, marking the staurolite isograd and zone (Hess, 1969; Carmichael, 1970; Novak and Holdaway, 1981). However, here staurolite does not appear until higher, within the andalusite-cordierite-biotite zone, and is bulk compositionally controlled, reflecting, where present, a more iron- and aluminum-rich composition.

According to Hess' (1969; fig. 6) petrogenetic grid, the transition from the garnet zone to the andalusite-cordierite-biotite zone (figs. 5A and 5B) should involve the following sequence of discontinuous reactions (see also Thompson, 1976):

$$Gt + Chl + Mu = St + Bt + Qtz + W, \quad (3)$$

$$St + Chl + Mu = Bt + And + Qtz + W, \quad (4)$$

$$Chl + Mu + Qtz = Bt + Crd + And + W. \quad (5)$$

The assemblage chlorite-biotite-cordierite is listed by Hess (1969) as an assemblage that may be compatible with the products of reaction (4), and thus it could be compatible with andalusite-biotite assemblages. However, here andalusite occurs first with cordierite-biotite (reaction 5), and the assemblage chlorite-biotite-cordierite would be eliminated by this reaction. The assemblage biotite-cordierite-andalusite (table 6) is given by Hess (fig. 6) as a possible product

Table 4. Statistical comparison of metamorphosed coarse- and fine-grained rocks of the Sitka Graywacke, southern Baranof Island, Alaska

[Specimen 79DB178B (table 3) was not included in the statistical calculations because it was determined petrographically to have been a sandstone originally, not a mudstone like the other fine-grained specimens. Number of coarse-grained samples is 10, and of fine-grained samples is 9. Geometric mean for semiquantitative spectrographic results rounded to appropriate units; major elements in weight percent; minor elements in parts per million]

	Range		Median		Mean		Standard deviation	
	Coarse	Fine	Coarse	Fine	Coarse	Fine	Coarse	Fine
SiO_2....	65.97-71.69	59.36-63.61	69.06	60.04	68.87	61.20	1.80	1.50
Al_2O_3...	13.38-15.78	16.88-18.97	14.74	17.87	14.84	18.00	.71	.67
Fe_2O_3...	.47- .87	.61- 1.13	.67	.85	.67	.88	.14	.16
FeO.....	2.81- 4.34	4.18- 5.64	3.63	5.22	3.50	5.06	.50	.44
MgO.....	1.54- 2.44	2.68- 3.49	2.01	2.97	1.99	2.96	.34	.22
CaO.....	1.69- 2.91	2.00- 3.00	2.18	2.46	2.19	2.45	.33	.31
Na_2O....	1.88- 4.09	2.29- 3.60	3.58	2.64	3.47	2.71	.60	.35
K_2O.....	1.82- 3.81	2.38- 4.39	2.24	3.41	2.32	3.38	.57	.56
TiO_2....	.49- .75	.75- .91	.55	.80	.58	.81	.09	.05
P_2O_5....	.10- .15	.13- .21	.11	.18	.12	.18	.02	.03
MnO.....	.05- .08	.07- .12	.07	.09	.06	.09	.02	.02
B.....	2-20	7-70	10	30	7	30		
Ba.....	500-1500	700-1500	700	1000	700	1000		
Be.....	1-2	.7-1.5	1	1	1	1		
Co.....	7-20	7-30	10	15	10	15		
Cr.....	20-50	30-70	30	50	30	50		
Cu.....	10-50	30-70	20	70	20	50		
Ga.....	20-30	20-30	20	30	20	30		
La.....	30-70	20-70	50	50	50	50		
Mn.....	300-1000	500-1500	500	700	500	700		
Nb.....	7-20	10-15	15	10	15	10		
Ni.....	7-30	10-50	15	20	15	20		
Pb.....	20-50	20-50	30	30	30	30		
Sc.....	10-20	15-30	15	20	15	20		
Sn.....	2-5	2-7	3	3	3	3		
Sr.....	300-700	200-300	300	300	300	300		
V.....	100-200	150-200	150	200	150	200		
Y.....	15-20	15-30	15	15	15	20		
Yb.....	2-3	2-5	2	2	2	3		
Zn.....	70-150	70-200	100	100	100	100		
Zr.....	70-200	70-200	100	100	100	100		

of reaction (5), which models the disappearance of chlorite (Burnell and Rutherford, 1984). Reactions (4) and (5) may have occurred simultaneously on southern Baranof Island (see the section "Discussion").

The sillimanite isograd is marked by the first appearance of sillimanite (fibrolite) and the disappearance of staurolite (figs. 5B and 5C); the isograd is based on the reaction

$$\text{And} = \text{Sill}. \qquad (6)$$

The disappearance of staurolite can be modeled by the following discontinuous reaction from Thompson (1976; see also, Hess, 1969):

$$\text{St} + \text{Mu} + \text{Qtz} = \text{Gt} + \text{Sill} + \text{Bt} + \text{W}. \qquad (7)$$

This reaction may have proceeded simultaneously with reaction (6). For the details of the transition from the staurolite zone to the sillimanite zone in similar (but not identical) rocks and conditions, see Guidotti (1974). In the sillimanite zone, sillimanite occurs mostly as fibrolite needles on biotite, and it is the only Al_2SiO_5 mineral present in most specimens. Only a few specimens contain both andalusite and sillimanite, and in these andalusite occurs as separate porphyroblasts not in contact with the fibrolite, which tends to be associated with biotite.

These andalusite and sillimanite occurrences may be interpreted in two ways: (1) the rocks attained the pressure-temperature (P-T) conditions of the sillimanite stability field, and andalusite is an unstable mineral, or (2) fibrolite crystallized metastably at a lower temperature in the andalusite field (fig. 6).

The first interpretation is supported by Holdaway's (1971) experimental evidence that fibrolite, which he considers to be metastable, raises the andalusite-sillimanite boundary about 100 °C higher than that determined by Weill (1966). He states that in order to form fibrolite from andalusite, 200 °C or more of overstepping is required, whereas to form fibrolite from muscovite dehydration would require no

Table 5. Garnet and whole-rock analyses of schists from the metamorphosed Sitka Graywacke, southern Baranof Island, Alaska

[Garnet analyses (in weight percent) by H.N. Elsheimer, C.O. Ingamells, M. Cremer (H_2O), S. Neil (FeO), and R.E. Mays (TiO_2); rapid rock analyses by P. Elmore, S. Botts, L. Artis, and H. Smith; n, index of refraction; D, density (in grams/cubic centimeter); a, unit cell (in angstroms); garnet end-member molecules (in percent) after Rickwood (1968)

	Garnets			Whole rock		
Sample No...	62ABd147	62ABd149	62ABd152	62ABd147	62ABd149	62ABd152
SiO_2.....	36.9	36.9	37.1	66.2	55.5	62.7
Al_2O_3.....	20.6	20.5	20.6	14.3	20.0	16.7
Fe_2O_3.....	1.96	6.69	4.36	1.3	1.0	.83
FeO.....	24.58	27.63	27.64	5.4	7.3	4.7
MgO.....	2.0	3.8	3.9	2.1	3.8	3.2
CaO.....	5.6	1.2	2.2	2.8	2.6	2.5
Na_2O.....	.06	.03	.02	2.4	3.9	3.3
K_2O.....	.05	.04	.01	2.5	2.5	2.8
Total H_2O.....	.01	.10	.00	1.39	2.44	1.82
TiO_2.....	.15	.12	.15	.77	1.1	.80
P_2O_5.....	.01	.03	.01	.30	.22	.28
MnO.....	7.6	2.1	3.1	.53	.16	.11
CO_2.....	--	--	--	.08	.06	.10
Total	99.52	99.14	99.09	100.07	100.58	99.84
n	1.805	1.804	1.805			
D	4.10	4.19	4.15			
a	11.5922	11.5326	11.5439			
End-member molecules						
Andradite	1.4	1.3	.9			
Pyrope	8.1	15.5	15.8			
Spessartine	17.4	4.9	7.1			
Grossular	14.4	2.0	5.1			
Almandine	58.3	76.1	70.7			
Schorlomite	.4	.2	.4			

Sample descriptions:
62ABd147 Garnet-biotite semischist Gz(L4) zone, Larch Bay, Baranof Island.
62ABd149 Garnet-biotite schist ACz(H1) zone, Larch Bay, Baranof Island.
62ABd152 Garnet-biotite schist ACz(H1) zone, Larch Bay, Baranof Island.

more than 9 °C of overstepping. Thus, according to Holdaway (1971) it is more common to grow fibrolite on micas upon heating while andalusite in the same rock breaks down. According to these data, the presence of fibrolite in the aureoles should indicate that the rocks have attained at least the temperature range of the sillimanite field.

The second interpretation is based mainly on Hollister's (1969) work on the field relations in the contact metamorphic terrane of the Kwoiek area of British Columbia. In this terrane, both fibrolite and coarse-grained sillimanite occur. The fibrolite developed on biotite and andalusite, whereas sillimanite developed from kyanite. Hollister concludes that fibrolite formed at a lower temperature than the coarse-grained sillimanite, probably metastably in the andalusite stability field. This interpretation is counter to Holdaway's (1971) evidence that an overstepping of temperature is necessary for the andalusite-fibrolite transition.

In summary, we favor interpretation (1) because Holdaway's (1971) mineral assemblages and textural relations are closer to those at southern Baranof Island than are those of Hollister (1969) at Kwoiek. The latter, especially the presence of kyanite, seem more complex and seem to represent higher pressure metamorphism. Finally, we use "sillimanite" for fibrolite in comparing mineral assemblages of southern Baranof Island with those of other metamorphic facies series, no ambiguities have been noted, and our mineral assemblages are those to be expected in sillimanite-bearing rocks.

A mineralogic characteristic of the sillimanite zone is the appearance of orthoclase accompanied by a decrease in muscovite (table 6). (This isograd is not shown on figure 3.) This finding suggests that at least part of the sillimanite zone exceeded the temperature for the initiation of the reaction (Storre, 1972)

$$Mu + Qtz = Kspar + Sill + W. \quad (8)$$

Table 6. Observed mineral assemblages in the pelitic metamorphic rocks of southern Baranof Island appropriate to the AFM projection (fig. 5)

[All assemblages contain quartz and muscovite, and a few may also contain orthoclase, indicated (Or). Chl, chlorite; Bt, biotite; Gt, almandine-rich garnet; St, staurolite, Crd, cordierite; And, andalusite; Sill, sillimanite]

Garnet zone	Sillimanite zone
Chl-Bt	Bt-Sill (Or)
Bt-Gt	Bt-Crd (Or)
Chl-Bt-Gt	Bt-Gt-Sill (Or)
Chl-Bt-Crd	Bt-Gt-And-Sill
Andalusite-cordierite-biotite zone	**Garnet-cordierite zone**
Bt-And	Bt-Gt-Crd-Sill (Or)
Bt-Crd-And	
Bt-Gt	
Bt	
Crd	
Bt-Gt-St	
Bt-St-And	

A mineral assemblage indicative of a zone higher than the sillimanite zone, the garnet-cordierite zone, occurs in migmatitic gneiss in a small roof pendant near the northeast contact of the Crawfish Inlet pluton, about 5 km south of the head of Gut Bay (GCz, fig. 3). The gneiss contains, in addition to muscovite, orthoclase, and quartz, the assemblage biotite-garnet-cordierite-sillimanite. When plotted on the AFM diagram (projected from potassium feldspar), the garnet-cordierite tieline breaks the sillimanite-biotite tieline and defines the garnet-cordierite isograd (dashed line, fig. 5D). According to Thompson (1976, fig. 3b) garnet-cordierite-potassium feldspar is the high-temperature product of the discontinuous reaction

$$Bt + Sill = Gt + Crd + Kspar. \quad (9)$$

The presence of the four-phase assemblage (table 6) suggests an incomplete reaction, but the assemblage might also be due to substitution by other components (particularly in the garnet) or by the X_{H_2O} being buffered by the reaction.

DISCUSSION

The sequence of mineral assemblages in the southern Baranof Island thermal aureoles can be plotted with good agreement on Hess' (1969) petrogenetic grid, which was constructed for similar pelitic rocks (fig. 6). A P-T gradient was established for the Baranof facies series by finding the appropriate mineral assemblages on his grid. Hess, in plotting the

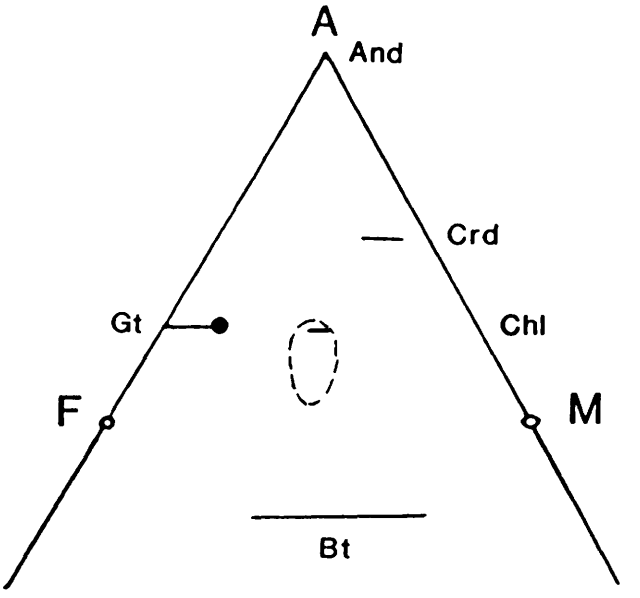

Figure 4. Schematic AFM projection (projected from muscovite) showing composition of analyzed garnet (black dot includes specimens 62ABd149 and 62ABd152, table 5), adjusted bulk compositions (see text) of pelitic rocks (dashed line encloses field of 13 analyses, tables 3 and 5), and estimated compositions of other important mineral phases. See table 6 for abbreviations.

P-T gradient for the Pyrenean facies series, states that the absence of the chlorite-biotite-andalusite assemblage requires that the gradient passes on the low-pressure side of the invariant point (G,H). The Baranof rocks also lack the chlorite-biotite-andalusite assemblage, but the disappearance of chlorite is accompanied by the appearance of the assemblage andalusite-cordierite-biotite instead of staurolite-biotite-cordierite and suggests that the P-T gradient passes on the high-pressure side of (G,H). How far above (G,H) is uncertain; it depends on whether the reactants of reaction (4) are absent because the gradient lies close to (G,H), or because of inappropriate bulk composition. The Baranof gradient shown is based on the first assumption; if the second obtained, the curve would be higher and the slope more like that of the Pyrenean facies series.

The low end of the Baranof gradient lies in the P-T field in which the mineral assemblage found in the garnet zone, garnet+chlorite, is stable (fig. 6).

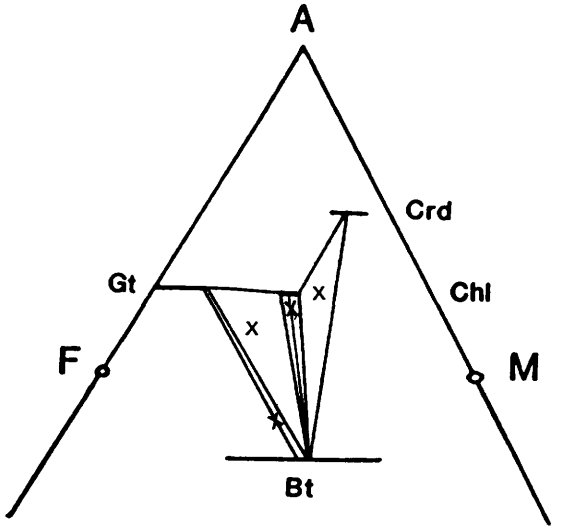

A. Garnet zone (L4)

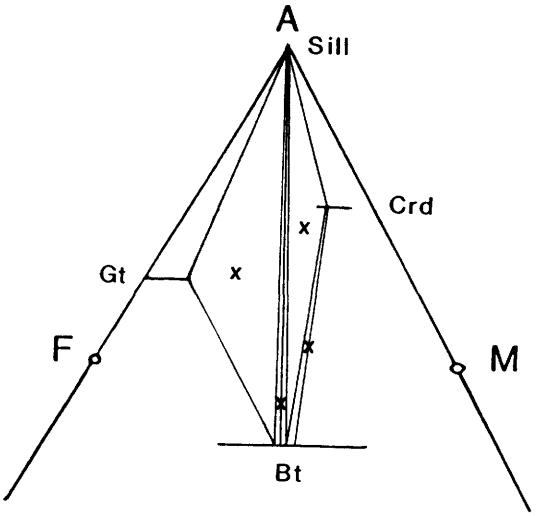

C. Sillimanite zone (H3)

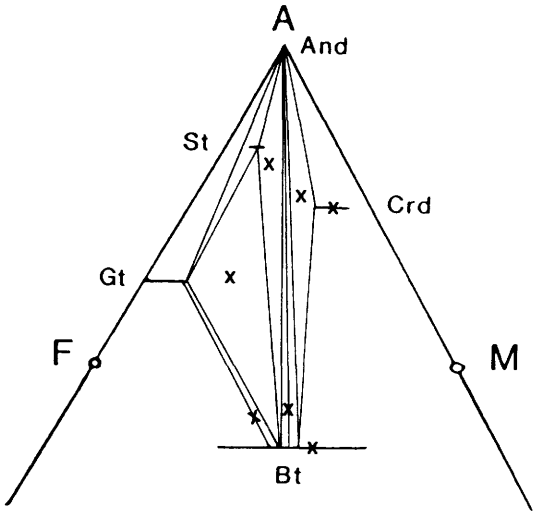

B. Andalusite-cordierite-biotite zone (H1 and H2)

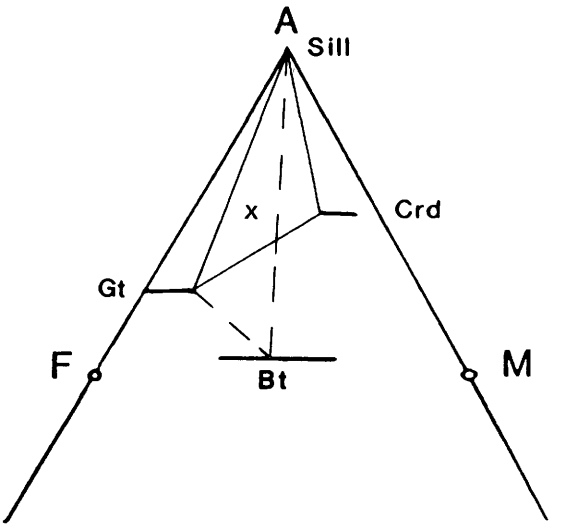

D. Garnet-cordierite zone

Figure 5. Schematic AFM diagrams based on mineral assemblages in pelitic metamorphic rocks listed in table 6. Dashed lines indicate existence of four-phase assemblages; X marks observed assemblages. All assemblages include quartz and muscovite. Figure 5D projected from orthoclase; all others from muscovite. See table 6 for abbreviations. Zone designations L4, H1, H2, and H3 refer to table 1.

According to Hess, the associated assemblage chlorite-biotite-cordierite is stable in this field.

Proceeding upgrade on the grid, the gradient cuts the boundary represented by reaction (3) in which the garnet-biotite tieline is broken and the staurolite-chlorite tieline is formed (staurolite isograd). However, on Baranof Island staurolite appears to be absent at this point, and instead andalusite appears, accompanied by cordierite-garnet, the products of reaction (5) (andalusite-cordierite-biotite isograd). As noted previously, reaction (3) probably did not occur because of inappropriate bulk composition. This may also be the reason why the products of reaction (4) seem to be absent, but if the P-T gradient lies close to (G,H) (fig. 6), the P-T field of this reaction would be very small. Since reaction (5) is a terminal reaction for chlorite, the nearly simultaneous appearance of andalusite and disappearance of chlorite is further evidence that reaction (5) is responsible for the appearance of andalusite.

The first appearance of staurolite in the upper part of the andalusite-cordierite-biotite zone does not correspond to a specific reaction in that region of Hess' grid; instead it lies in the large P-T field in which the assemblages biotite-staurolite-andalusite and biotite-garnet-staurolite are stable. It is likely that reaction (3) did not occur, and hence the staurolite isograd is not seen because of inappropriate bulk composition.

Sillimanite appears and staurolite disappears nearly simultaneously, and thus the P-T gradient must pass near the intersection of the boundary between the andalusite and sillimanite fields and the staurolite-out reaction curve (reaction (7)). This control point

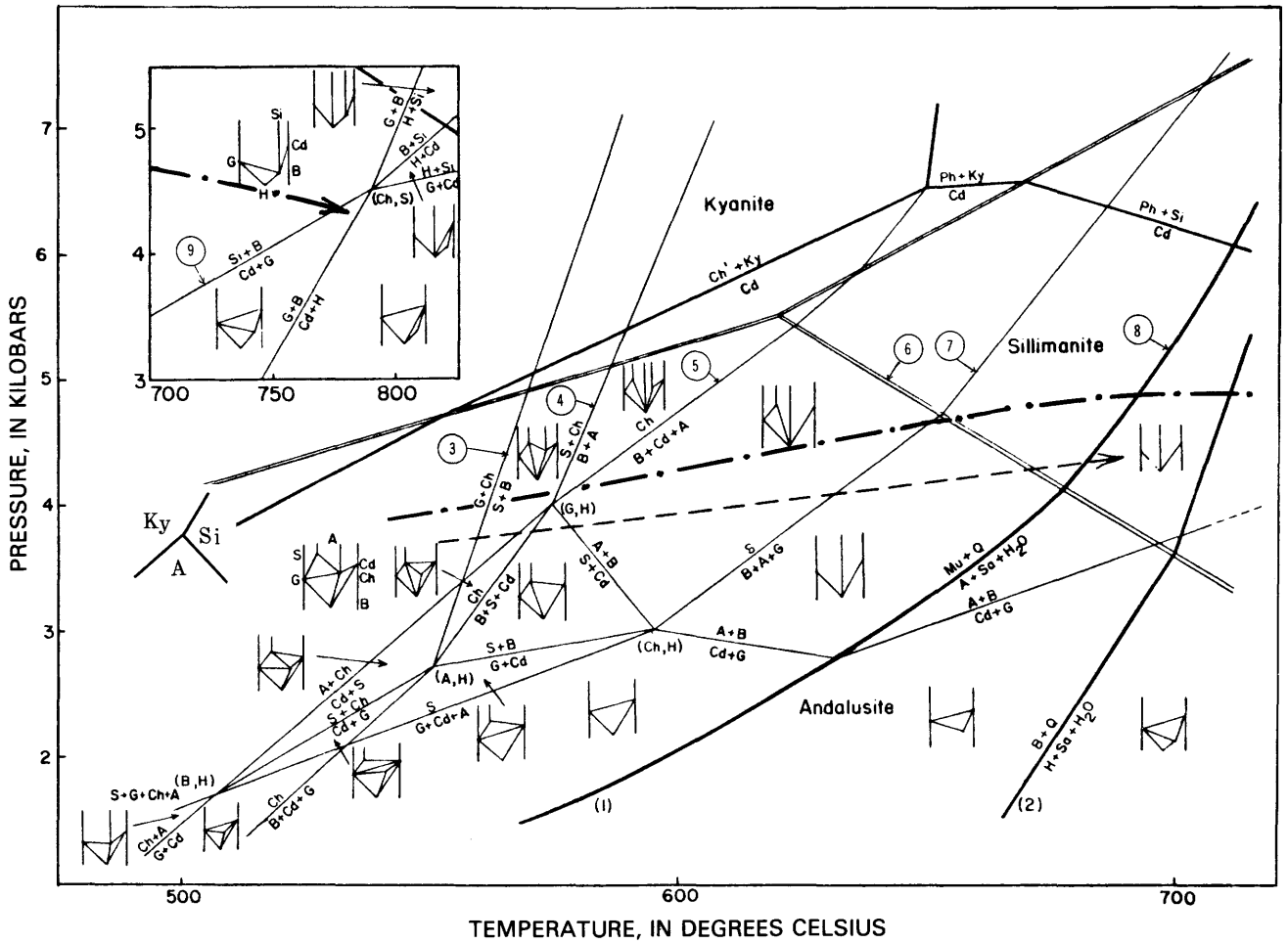

Figure 6. Petrogenetic grid for muscovite-quartz- and potassium feldspar-quartz-bearing systems (modified from Hess, 1969, fig. 3). Ky, Si, and A indicate position of alternative Al_2SiO_5 triple point from Holdaway (1971); dash-dot arrow, pressure-temperature gradient of Baranof facies series; circled numbers refer to reactions in text; dashed arrow, pressure-temperature gradient of Pyrenean facies series; double lines, Al_2SiO_5 equilibria; heavy lines, equilibria in Fe-free system, reaction (1), and Fe-bearing system, reaction (2); light lines, calculated equilibria; insert shows invariant point (Ch,S) on univariant line marked by equilibrium A + B = Cd + G. A, andalusite; B, biotite; Ch, chlorite; Ch', Mg-chlorite; Cd, cordierite; G, garnet; H, hypersthene; Ky, kyanite; Mu, muscovite; ph, phlogopite; Q, quartz; Sa, sanadine; Si, sillimanite; S, staurolite. Small unlabeled diagrams indicate AFM fields and tielines present in different parts of the grid.

requires a steeper P-T gradient than that of the Pyrenean facies series. If the disappearance of staurolite is bulk compositionally controlled and occurs before the staurolite-out reaction curve, then the gradient would have to be even steeper in order to reach the sillimanite field.

The next reaction from the grid that is recognized is the muscovite-out reaction (8). This is manifest by a decline in muscovite and an increase in orthoclase in the sillimanite zone and higher (table 6). The reaction places only a broad control on the position of the P-T gradient in the grid (fig. 6).

The highest grade assemblage, biotite-garnet-cordierite-sillimanite, corresponds to Hess' high-temperature reaction, producing cordierite-garnet (reaction (9)) on the low-pressure side of the invariant point (Ch,S). This assemblage controls the high-temperature end of the Baranof P-T gradient, but a negative slope is needed in order to reach this field. Whether or not this reflects a real decrease in pressure is unknown, but Gil Ibarguchi and Martinez (1982) report a decrease in both pressure and temperature in the highest zone, possibly due to late deformation. Overall, the Baranof P-T gradient ranges in temperature from 550 to 790 ^{o}C and in pressure from 3.9 to 4.75 kbars (fig. 6). The pressure decreases above 700 ^{o}C, attaining a value of about 4.4 kbars in the cordierite-garnet field at 790 ^{o}C.

As indicated by the foregoing discussion, the petrogenetic grid of Hess (1969) seems internally consistent with regard to the sequence of metamorphic mineral assemblages from southern Baranof Island. However, the position of the grid in P-T space is another matter. This is discussed here because it indicates the uncertainty that attends the use of petrogenetic grids, regardless of whether generalized or specific mineral composition data are used. One of the principal P-T controls of the grid is the system kyanite-andalusite-sillimanite of Richardson and others (1969), the triple point of which is at 5.5 kbars and 622 ^{o}C. It is well known, however, that values for this triple point obtained by various workers have ranged widely. For example, the triple point of Holdaway (1971), which has been favored in more recent papers (Holdaway, 1978; Anderson and others, 1977; Day and Kumin, 1980; Grambling, 1981; Hodges and Spear, 1982), is located at 3.75 kbars and 501 ^{o}C (fig. 6). The use of this triple point to control the grid would considerably lower both the temperature and the pressure values in the grid.

Another P-T control on the grid concerns the formation of cordierite. As mentioned in the descriptions of the mineral assemblages, recent workers have studied the reactions involving cordierite with variable results. Burnell and Rutherford (1984) experimentally produced the terminal reaction for chlorite (reaction (5)) and obtained data that constrained the univariant assemblage chlorite-cordierite-biotite Al_2SiO_5 as lying between points 640 ^{o}C at 4 kbars and 612 ^{o}C at 2 kbars. Although these pressures are comparable to those on the grid, the temperatures are much higher than those for the chlorite-bearing assemblages (fig. 6).

The widespread occurrence of the assemblage cordierite-almandine rich garnet-sillimanite is possible only at high temperatures and at a restricted range of intermediate pressures (Wynne-Edwards and Hay, 1963; Winkler, 1979, p. 230). The reaction through which cordierite is converted to garnet, sillimanite, and quartz is pressure sensitive, and the Mg content of cordierite should be a good geobarometer (Martignole and Nantel, 1982, p. 313). However, cordierite has two properties for which the effects on the reaction have not been properly evaluated. These are (1) the effects of water activity related to the variable hydration of cordierite, and (2) the effects of cordierite order/disorder (Essene, 1982, p. 180-181). The experimental and theoretical models proposed by various workers do not agree by wide margins. However, the models based on the experiments of Holdaway and Lee (1977) and those based on the calculations by Newton and Wood (1979) and Martignole and Sisi (1981) do agree approximately on pressures for intermediate values of water pressure; the pressures for intermediate Fe-Mg cordierite range from 3.25 to 3.7 kbars for 650 ^{o}C. These pressures and temperatures are lower than those of the grid.

In contrast, the pressure calculations of Gil Ibarguchi and Martinez (1982), based on compositions of garnet, biotite, and cordierite from the garnet-cordierite-sillimanite gneisses in the Iberian Massif, Spain, are generally higher, ranging from 4 to 7 kbars. These variations resulted from using different geobarometers and different assumptions. Using the Newton and Wood (1979) garnet-cordierite geobarometer, Gil Ibarguchi and Martinez found pressures ranging from 4 kbars ($P_{H_2O} = 0$) to 5 kbars ($P_{H_2O} = P_t$). They state that their most reliable result came from calculating the P-T conditions, using the experimental data of Holdaway and Lee (1977), for the coexistence of the seven-phase assemblage in the following reaction:

$$Bt + Sill + Gt + Qtz = Crd + Kspar + W, \qquad (10)$$

which yielded 4.3 kbars, 695 ^{o}C for $X_{H_2O} = 0.5$. This pressure is close to the value 4.4 kbars (at 790 ^{o}C) for the garnet-cordierite field at the upper end of the Baranof P-T gradient on Hess' grid (fig. 6).

It should be obvious from the above discussion that no general solution to the P-T petrogenetic grid problem is at hand. The pressures obtained by the various workers for the garnet-cordierite-sillimanite assemblage range from 3.5 to 7.0 kbars, about equivalent to 11 to 25 km depth. Most of the calculated pressures are more in harmony with the higher pressures of Hess' (1969) grid than the lower ones that would be produced if his grid were readjusted by using the lower triple point of Holdaway (1971). The best conclusion is that of Hess (1969), that the value of the petrogenetic grid is not found in the pressure-temperature estimates of the various facies but in the systematic analysis of various facies series, based on certain critical mineral assemblages.

Finally, in Loney and others (1975, p. 90) it was stated that the experimental evidence, largely from Al_2SiO_5 triple points, indicates a deeper minimum depth of metamorphism (11 km) of the type on Baranof Island than does field evidence for the depth of the overburden (3 km). Although the present analysis is based on a different approach, this statement still holds.

SUMMARY

1. The Sitka Graywacke in which the contact aureoles were developed consists dominantly of interbedded semipelitic metagraywacke and pelitic metamudstone with a consistent composition throughout the aureoles.

2. The intrusion of the Tertiary plutons that produced the contact aureoles in southern Baranof Island was postkinematic and passive. The metamorphic rocks underlie an area of at least 1,200 km^2 and are the result of a single episode of thermal metamorphism. An initial and unexposed stage of the intrusive episode may have occurred during the last phase of intense folding (F_2) that affected Baranof Island in general.

3. The previously mapped metamorphic zones and their boundaries (Loney and others, 1975; table 1) have been evaluated relative to model reactions using AFM projections and found to correspond to now-accepted reaction isograds. The boundary of the staurolite zone was determined to be bulk compositionally controlled and is not a reaction isograd.

4. The sequence of mineral assemblages in the aureoles shows good agreement with Hess' (1969) petrogenetic grid, on which we define a P-T gradient that ranges from about 3.9 kbars at 550 °C in the garnet zone, through a maximum pressure point of about 4.9 kbars at 690 °C in the sillimanite zone near the muscovite-out reaction curve, and ending at about 4.4 kbars at 790 °C in the garnet-cordierite zone (fig. 6). The Baranof P-T gradient as defined by Hess' (1969) grid represents depths of metamorphism ranging from 13.6 to 15.4 km.

REFERENCES CITED

Anderson, P.A.M., Newton, R.C., and Kleppa, O.J., 1977, The enthalpy change of the andalusite-sillimanite reaction and the Al_2SiO_5 diagram: American Journal of Science, v. 277, p. 585-593.

Burnell, J.R., Jr., and Rutherford, M.J., 1984, An experimental investigation of the chlorite terminal equilibrium in pelitic rocks: American Mineralogist, v. 69, p. 1015-1024.

Carmichael, D.M., 1970, Intersecting isograds in the Whetstone Lake area, Ontario: Journal of Petrology, v. 11, p. 147-181.

Chakraborty, K.R., and Sen, S.K., 1967, Regional metamorphism of pelitic rocks around Kandra, Singhbhum, Bihar: Contributions to Mineralogy and Petrology, v. 16, p. 210-232.

Day, H.W., and Kumin, H.J., 1980, Thermodynamic analysis of the aluminum silicate triple point: American Journal of Science, v. 280, p. 265-287.

Essene, E.J., 1982, Geologic thermometry and barometry, chap. 5 in Ferry, J. M., ed., Characterization of metamorphism through mineral equilibria: Reviews in Mineralogy, v. 10, p. 153-206.

Gil Ibarguchi, J.I., and Martinez, F.J., 1982, Petrology of garnet-cordierite-sillimanite gneisses from the El Tormes thermal dome, Iberian hercynian foldbelt (W Spain): Contributions to Mineralogy and Petrology, v. 80, p. 14-24.

Grambling, J.A., 1981, Kyanite, andalusite, sillimanite, and related mineral assemblages in the Truchas Peaks region, New Mexico: American Mineralogist, v. 66, p. 702-722.

Guidotti, G.V., 1974, Transition from staurolite to sillimanite zone, Rangeley quadrangle, Maine: Geological Society of America Bulletin, v. 85, p. 475-490.

Hess, P.C., 1969, The metamorphic paragenesis of cordierite in pelitic rocks: Contributions to Mineralogy and Petrology, v. 24, p. 191-207.

Hodges, K.V., and Spear, F.S., 1982, Geothermometry, geobarometry and the Al_2SiO_5 triple point at Mt. Moosilauke, New Hampshire: American Mineralogist, v. 67, p. 1118-1134.

Holdaway, M.J., 1971, Stability of andalusite and the aluminum silicate phase diagram: American Journal of Science, v. 271, p. 97-131.

____1978, Significance of chloritoid-bearing and staurolite-bearing rocks in the Picuris Range, New Mexico: Geological Society of America Bulletin, v. 89, p. 1404-1414.

Holdaway, J.M., and Lee, S.M., 1977, Fe-Mg cordierite stability in high-grade pelitic rocks based on experimental, theoretical, and natural observations: Contributions to Mineralogy and Petrology, v. 63, p. 175-198.

Hollister, L.S., 1969, Metastable paragenetic sequence of andalusite, kyanite, and sillimanite, Kwoiek area, British Columbia: American Journal of Science, v. 267, p. 352-370.

Loney, R.A., Brew, D.A., and Lanphere, M.A., 1967, Post-Paleozoic radiometric ages and their relevance to vault movements, northern southeastern Alaska: Geological Society of America Bulletin, v. 78, p. 511-526.

Loney, R.A., Brew, D.A., Muffler, L.J.P., and Pomeroy, J.S., 1975, Reconnaissance geology of Chichagof, Baranof, and Kruzof Islands, southeastern Alaska: U.S. Geological Survey Professional Paper 792, 97 p.

Martignole, J., and Nantel, S., 1982, Geothermobarometry of cordierite-bearing metapelites near the Morin anorthosite complex, Grenville province, Quebec: Canadian Mineralogist, v. 20, p. 307-318.

Martignole, J., and Sisi, J.C., 1981, Cordierite-garnet-H_2O equilibrium: A geological thermometer, barometer and water fugacity indicator: Contributions to Mineralogy and Petrology, v. 77, p. 38-46.

Mehnert, K.R., 1969, Composition and abundance of common metamorphic rock types, chap. 9 in Wedepohl, K.H., ed., Handbook of Geochemistry: Berlin, Springer-Verlag, v. 1, p. 212-296.

Meyers, A.T., Havens, R.G., and Dunton, D.J., 1961, A spectrochemical method for the semiquantitative analysis of rocks, minerals, and ores: U.S. Geological Survey Bulletin 1084-I, p. 1207-1229.

Miyashiro, A., 1973, Metamorphism and metamorphic belts: New York, John Wiley, 492 p.

Newton, R.C., and Wood, B.J., 1979, Thermodynamics of water in cordierite and some petrologic consequences of cordierite as a hydrous phase: Contributions to Mineralogy and Petrology, v. 68, p. 391-405.

Novak, J.M., and Holdaway, M.J., 1981, Metamorphic petrology, mineral equilibria, and polymetamorphism in the August quadrangle: American Mineralogist, v. 66, p. 51-69.

Richardson, S.W., Gilbert, M.C., and Bell, P.M., 1969, Experimental determination of kyanite-andalusite and andalusite-sillimanite equilibria: the aluminum silicate triple point: American Journal of Science, v. 269, p. 259-272.

Rickwood, P.C., 1968, On recasting analyses of garnet into end-member molecules: Contributions to Mineralogy and Petrology, v. 18, p. 175-198.

Storre, Bernhard, 1972, Dry melting of muscovite + quartz in the range P_s = 7 kb to P_s = 20 kb: Contributions to Mineralogy and Petrology, v. 37, p. 87-89.

Thompson, A.B., 1976, Mineral reactions in pelitic rocks: I. Prediction of P-T-X(Fe-Mg) phase relations: American Journal of Science, v. 276, p. 401-424.

Thompson, J.B., Jr., 1957, The graphical analysis of mineral assemblages in pelitic schists: American Mineralogist, v. 42, p. 842-858.

Turner, F.J., 1981, Metamorphic petrology--mineralogical, field, and tectonic aspects: New York, McGraw-Hill, 524 p.

Weill, D.F., 1966, Stability relations in the Al_2O_3-SiO_2-Na_3AlF_6 system: Geochimica et Cosmochimica Acta, v. 30, p. 223-237.

Williams, Howel, Turner, F.J., and Gilbert, C.M., 1954, Petrography--an introduction to the study of rocks in thin section: San Francisco, W.H. Freeman, 406 p.

Winkler, H.G.F., 1979, Petrogenesis of metamorphic rocks (5th ed.): New York, Springer-Verlag, 348 p.

Wynne-Edwards, H.R., and Hay, P.W., 1963, Coexisting cordierite and garnet in regionally metamorphosed rocks from the Westport area, Ontario: Canadian Mineralogist, v. 7, p. 453-478.

Zuffa, G.G., Nilsen, T.H., and Winkler, G.R., 1980, Rock-fragment petrography of the Upper Cretaceous Chugach terrane, southern Alaska: U.S. Geological Survey Open-File Report 80-713, 28 p.

GPO 785-048/48052